INTERFACIAL APPROACH OF DELAMINATION: POSSIBILITIES AND DIFFICULTIES

V. Albouys[1], O. Allix[2] , P. Ladevèze[2] & D. Lévêque[2]

[1] *CNES - Centre Spatial de Toulouse*
18, Av. Edouard Belin - 31055 TOULOUSE CEDEX
[2] *L.M.T., E.N.S. de Cachan / C.N.R.S. / Univ. P. et M. CURIE*
61, avenue du PrÄsident Wilson, 94235 CACHAN, FRANCE

SUMMARY : For the prevision of delamination a previously defined Damage Meso-Modeling of composite laminates is used. The interlaminar interfacial deterioration as well as the main inner lyer damage mechanisms are included. Attention is focused herein on the modeling of the interlaminar connection as an elastic interfacial and damageable medium. The connection with Fracture Mechanics and the identification on an interface damage model devoted to the delamination prediction is also addressed possibilities and difficulties are discussed. Examples of comparison between simulation and experiments are included.

KEYWORDS: Damage Mechanics, Meso-Modelling, Delamination, Identification

INTRODUCTION

Delamination often appears as the result of interactions between different damage mechanisms inside composite laminates, such as fibre-breaking, transverse micro-cracking and the debonding of adjacent layers itself [1] [2]. The analysis of delamination is often split into the study of the onset of delamination and the analysis of the development of an existing delaminated area. Up until now, initiation analysis has involved empirical criteria such as point-stress or average-stress [3]. More predicting tools, based on edge effects analysis [4], or singularity computation [5], are used in order to allocate a greater or lesser delamination tendency to different stacking sequences. Most propagation studies on composite laminates involve extensions of Fracture Mechanics [6] [7] usually applied to metallic materials. Recently, some authors tried to extend Fracture Mechanics to the study of the onset of delamination. This was accomplished by the introduction of a minimum length required for the beginning of delamination development [8].

Our aim is to build a bridge between damage mechanics and delamination by including all the damage mechanisms in delamination analysis. Delamination often appears as the result of interactions between different damage mechanisms, such as fiber-breaking, transverse micro-cracking and debonding of the adjacent layers themselves [9] [10]. Thus a damage meso-modeling, proposed in [11] [12] and developed in [13] [14], which includes both inner layer damage mechanisms and interfacial ones is used

At the meso-level, the laminate is described as a stacking sequence of inelastic and damageable homogeneous layers throughout the thickness and of damageable interlaminar interfaces. The single-layer model being identified, the aim is to determine the properties of any structures regarding delamination by knowing only a few characteristics of the interface. The word interface denotes here a physical yet two-dimensional medium. At the present applications only concern static loading without buckling.
The single layer model and its identification, including damage (such as fiber-breaking, transverse cracking and deterioration of the fiber-matrix bond) and inelasticity, were previously developed [11],[13]. The interlaminar interface is a two-dimensional entity which ensures traction and displacement transfer from one ply to another. Its mechanical behaviour depends on the angles between the fibers of the two adjacent layers.
Here we pay special attention to the basic aspects of the interlaminar interface model: definition, debonding and sliding effects modeling, qualitative connection with "micro information" and questions concerning identification. Therefore results given in [15] [16] are detailed. A general discussion on the formulation of interfacial law can be found in [17]. The question of its identification is discussed in [18] [19]. We try to verify and improve the identification by means of comparison over the delaminated area for holed specimens submitted to tension. The difficulty, for identification purposes, is that, due to the complexity of the state of stress, the interpretation of the test requires complex computation. To accomplish this, a software developed at the Laboratory [20], which is devoted to the delamination analysis of laminate structures with an initially-circular hole, has been used.
Most of the tests presented in this work have been conducted at AÉROSPATIALE, Suresnes (France), with the same M55J/M18 high-modulus carbon-fibre/epoxy resin material. This material is used particularly in space applications because of its good mechanical properties and its dimensional stability. The single-layer model of this material was identified in an earlier work [21].
Difficulty concerns fracture simulation. It is now rather well-known that classical damage models present serious shortcomings. For example, they do not contain classical linear fracture mechanics, which is quite effective in many cases. One solution is provided by the localisation limiter concept introduced in [22] [23]. This is a regularisation procedure which introduces additional terms built either from a non-local approach or from a second gradient approach.
Our solution for composites and especially laminated structures is based on what we call a damage mesomodel. It is a semi-discrete model for which the damage state is locally uniform within the mesoconstituents [12] [24]. For laminates, it is uniform throughout the thickness of each single layer; as a complement, delay effects are introduced.

MESOMODELLINGOFLAMINATES

In our pragmatic approach, the characteristic length is the thickness of the plies. The meso-model is defined by means of two meso-constituents:

- the single layer,
- the interface, which is a mechanical surface connecting two adjacent layers and depending on the relative orientation of their fibres.

The damage mechanisms (Fiber ruptures, Matrix Cracking and Delamination) are taken into account by means of internal damage variables. A meso-model is then defined by adding another property: a uniform damage state is prescribed throughout the thickness of the elementary ply. This point plays a major role when trying to simulate a crack with a damage model. As a complement, delayed damage models are introduced. The single layer model has been previsouly developed including the non-linear repsonse in compression in the diretcion of the fiber [25]. In those papers, the damage related to out-of-plane stresses σ_{13}, σ_{23} and σ_{33}

has been taken into account only in the interface model. The study of the influence of the damage associated with out of plane stresses is in progress [26].

INTERFACE MODELING [11] [14] [19]

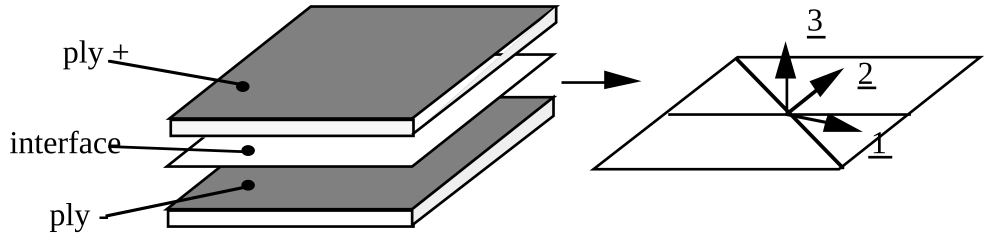

Fig. 1 : "Orthotropic" directions of the interface

The ideas and framework which govern the interface damage modeling are similar to those which are used for deriving the layer damage modeling [11],[13]. The effect of the deterioration of the interlaminar connection on its mechanical behaviour is taken into account by means of damage internal variables. The different damageable behaviour in "tension" and in "compression" are distinguished by splitting the strain energy into "tension-energy " and "compression-energy". More precisely we use the following expression of the energy per unit area:

$$E_D = \frac{1}{2}\left[\frac{<-\sigma_{33}>_+^2}{k^0} + \frac{<\sigma_{33}>_+^2}{k^0(1-d)} + \frac{\sigma_{32}^2}{k_2^0(1-d_2)} + \frac{\sigma_{31}^2}{k_1^0(1-d_1)}\right] \tag{1}$$

where k_i^0 is an interlaminar stiffness value and d_i the internal damage indicator associated with its Fracture Mechanics mode, while subscript i corresponds to an orthotropic direction of the interface (Figure 1), thus three internal damage indicators, associated with the three Fracture Mechanics modes are introduced.

Interfacial damage evolution laws

These evolution laws must satisfy the Clausius-Duheim inequality. Classically the damage energy release rates, associated with the dissipated energy ω,by damage and by unit area, are introduced:

$$Y_d = \frac{1}{2}\frac{<\sigma_{33}>_+^2}{k^0(1-d)^2} \; ; Y_{d_1} = \frac{1}{2}\frac{\sigma_{31}^2}{k_1^0\,(1-d_1)^2} \; ; Y_{d_2} = \frac{1}{2}\frac{\sigma_{32}^2}{k_2^0\,(1-d_2)^2} \tag{2}$$

with:

$$\omega = Y_d\,\dot{d} + Y_{d_1}\dot{d}_1 + Y_d\,\dot{d}_2 \quad (\,\omega \geq 0\,)$$

The following model, proposed in [15],[21], considers that the damage evolution is governed by means of an equivalent damage energy release rate of the following form:

$$\underline{Y}\,(t) = \sup_{\tau \leq t} < \Big[\,[\,(Y_d^\alpha + (\gamma_1 Y_{d_1})^\alpha + (\gamma_2 Y_{d_2})^\alpha)_{\tau}^{1/\alpha}] + \gamma <\sigma_{33}>_+ \Big] >_+ \tag{3}$$

this means that (i) the evolution of the damage indicators are assumed to be coupled (as for single layers) (ii) the damage evolution depends (mainly) on the maximal value of the equivalent damage energy release rate. γ_1, γ_2 γ and α are material parameters. In terms of delamination modes, the first term is associated with the first opening mode, and the two others are associated with the second and third modes. The parameter γ is introduced in order decrease the level of damage in the case of comparison.
A damage evolution law is then defined by the choice of a material function ω, such that :

$$d = d_1 = d_2 = \omega(\underline{Y}) \text{ if } d < 1;\ d = d_1 = d_2 = 1 \text{ otherwise}$$

a simple case, used for application, is:

$$\omega(\underline{Y}) = \left[\frac{n}{n+1}\,\frac{\langle \underline{Y} \rangle_+}{Y_c}\right]^n \tag{4}$$

where a critical value Y_c and are introduced. The high values of n case corresponds to brittle interface. To summarize, the damage evolution law is defined by means of six intrinsic material parameters Y_c, γ_1, γ_2, α and n. It is shown after that Y_c, γ_1, γ_2 and α. are related to the critical energy release rates. As regards the creation of a new delamination crack the significant parameters are n and α .

Links with Fracture Mechanics
A simple way of comparing Damage Mechanics with Linear Elastic Fracture Mechanics is to compare the mechanical dissipation yielded by the two approaches. This was performed in [15] [19], and only the results are presented below.
In the case of pure-mode situations, when the critical energy release rate reaches its stabilised value at the propagation denoted by G_c^p, we obtain:

$$G_{c\mathrm{I}}^p = Y_c\,;\quad G_{c\mathrm{II}}^p = \frac{Y_c}{\gamma_1}\,;\quad G_{c\mathrm{III}}^p = \frac{Y_c}{\gamma_2} \tag{5}$$

For a mixed-mode loading situation, we simply derive a standard LEFM model (Bathias 1995):

$$\left(\frac{G_\mathrm{I}}{G_{c\mathrm{I}}^p}\right)^\alpha + \left(\frac{G_\mathrm{II}}{G_{c\mathrm{II}}^p}\right)^\alpha + \left(\frac{G_\mathrm{III}}{G_{c\mathrm{III}}^p}\right)^\alpha = 1 \tag{6}$$

wherein α governs the shape of the failure locus in the mixed mode.

FRACTURE MECHANICS TESTS

Presentation of the tests
The tests of crack propagation in interlaminar fracture specimens are usually conducted on beam specimens with an initiated crack at the studied interface. Our specimens are 300 mm long and 20 mm wide. An anti-adhesive film 40 mm long and 25 μm in thickness is inserted at the mid-plane in order to initiate cracking. Each specimen tested is a $[(+\theta/-\theta)_{4s}/(-\theta/+\theta)_{4s}]$ laminate with θ= 0°, 22.5° or 45°, according to the three kinds of $\pm\theta$ interlaminar interfaces.

The stacking sequence is equilibrated and symmetric in each arm of the beam in order to suppress any bending/twisting coupling membrane. The mean thickness of a single ply is on the order of 0.1 mm.
The tests conducted in this work, which were developed at the AÄROSPATIALE facility in Suresnes (France) [27], are the pure-mode I DCB (Double-Cantilever Beam) Test [6], the pure-mode II ENF (End-Notched Flexure) test [7], and two mixed-mode tests: the MMF (Mixed-Mode Flexure) test [28] and the CLS (Cracked-Lap Shear) test [27]. The tests were conducted on an INSTRON testing machine at ambient temperature (about 25°C) and at an imposed displacement rate. The displacement rate was set at 2 mm min^{-1} in the DCB and CLS tests and at 1 mm min^{-1} in the ENF and MMF tests. In these two latter bending tests, the total useful length is 180 mm (only 100 mm for the ±45° ply-based laminate).

Results and non-standard analysis

The critical energy release rate G_c is classically obtained by deriving the compliance of the specimen, as is usually carried out within the concept of Linear Elastic Fracture Mechanics. This compliance can be analytically computed by use of the Classic Beam Theory, for instance. Here, we derive the critical rates from fitting the experimental compliance. This method is useful since it corrects the measured crack length, which is not easy to accomplish because of the difficulty in locating exactly the end of the crack on each side of the specimen. We applied this method to both the DCB and MMF tests.

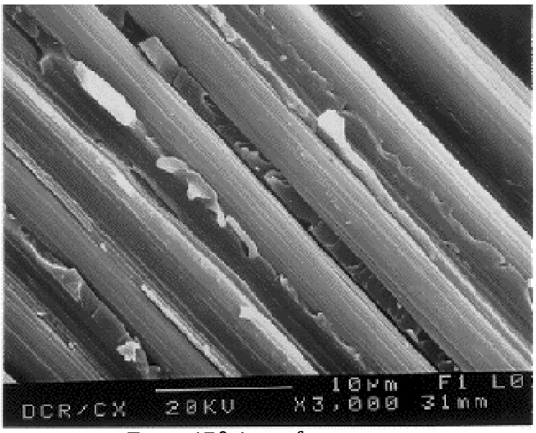

7a. ±45° interface case.

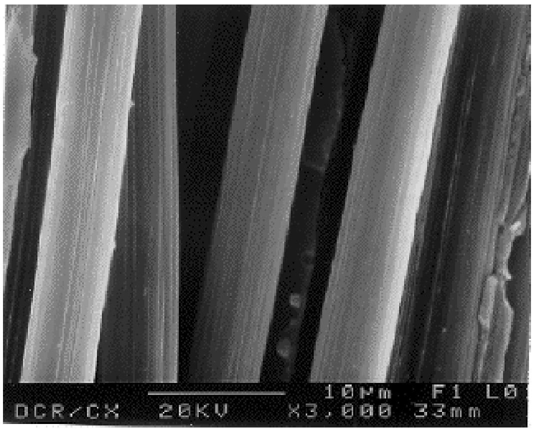

7b. 0°/0° interface case.

Fig. 2: Fractography of debonded interlaminar interfaces in mode I DCB test.

Previous studies [11] [15] [19] have highlighted the importance of taking into account the intralaminar damage for an accurate derivation and identification of the local energy release rate. Nevertheless, the portion of the energy dissipated in the layers was not identified. Here, this identification is performed in a simplified manner by making use of: (i) a two-dimensional elastic plate computation, and (ii) a local non-linear re-analysis using for the previously-identified single layer damage and inelastic model. The damage distribution in the laminate thickness is evaluated with the DAMLAM software, developed in the LMT Laboratory, from the data of the generalized loading (at each point of the plate) given by the 2D FE computation. Then, the portion of the energy dissipated inside the layers can be deduced. We found that this energy is significant only for the ±45° ply-based laminate in the case of the ENF, MMF and CLS tests.
From all the experimental points of three specimens for each test and for each stacking sequence, the mean critical energy release rates are derived and corrected by this method, as presented in Figure 3. From the corrected rates, it seems that the interfaces can be classified into two categories: the 0°/0° interface, whose critical energy release rates are always lower

than those of the disorientated-angle interfaces, and this latter kind of ±θ interface, whose critical rates seem to be independent of the angle value. This classification has a physical explanation since the ±θ interfaces are revealed by the wall effect between the fibers of adjacent layers [29], which is not the case for the 0°/0° interface. Moreover, fractographies of the delaminated interfaces show that the interlaminar resin plays a major part in the damage process of ±θ interfaces (Figure 2a), whereas massive full fiber-matrix debonding in the 0°/0° interface case can be observed (Figure 2b), which explains its rather brittle behaviour.

Identification of the propagation parameters

From the corrected critical energy release rates at propagation and from the relationships existing between Fracture Mechanics and Damage Mechanics [21] [22], we deduce the values of the critical energies Y_c and the coupling coefficient γ_1. Without any further information on mode III interlaminar fracture, we can choose $\gamma_2 = \gamma_1$, which is justified at least for a ±45° interface. The identification results are reported in Table 1 and Figure 3. For each kind of interface, the parameter α, which governs the shape of the failure locus in the mixed-mode, is identified in the normalized plane mode I/mode II (see Figure 4 for instance). It is observed that α is always greater than 1, and we can choose the same parameter α for the two ±θ interfaces ($\theta \neq 0°$).

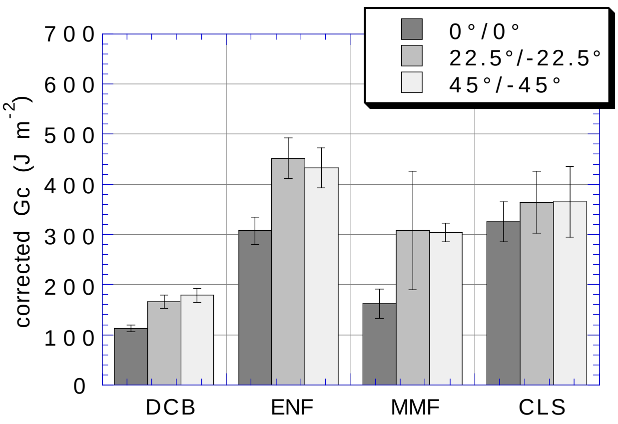

Fig. 3 : Critical energy release rates at propagation.

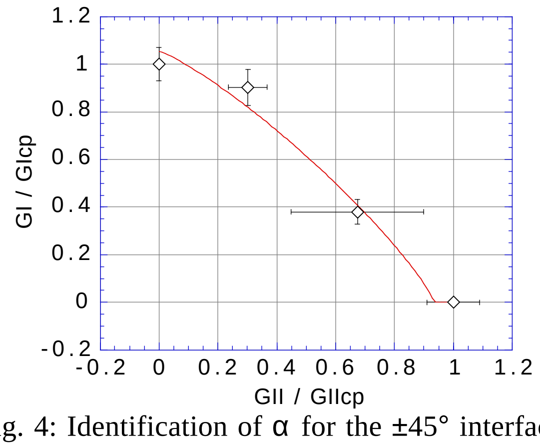

Fig. 4: Identification of α for the ±45° interface.

Table 1. Interface model parameters.

Interface	Y_c (N mm^{-1})	γ_1	α
0°/0°	0.113 ± 0.007	0.37 ± 0.15	1.59
±22.5°	0.167 ± 0.013	0.36 ± 0.17	1.12
±45°	0.192 ± 0.014	0.44 ± 0.16	1.19

EDGE DELAMINATION TENSION TESTS

Introduction

The experimental study of the initiation of delamination often requires EDT (Edge Delamination Tension) specimens [30]. Fracture Mechanics is not well-adapted for the analysis of such a test since the energy release rate vanishes at zero crack length. The meso-modeling concept is then useful when dealing with such a case.

During the initial stage, a review of many EDT tests in the literature has indicated the high frequency of superfluous tests in terms of the type of interface and loading mode [31]. For laminates containing some 90° plies, one pragmatic criterion for reducing the transverse cracking is to decrease the relative thickness of these plies [32]. Our laminates tested in tension are presented in Table 3. We can note that the 90°/90° interface is equivalent to a 0°/0° interface.

Experiments

The EDT specimens tested have 16 plies, and measure 30 mm in width and 150 mm in gage length. A bi-directional gage is fastened on each side of the specimen, and acoustic emission is used to detect the beginning of delamination. Optical observations of the edges and X-radiography serve to complete these tests. Each test is conducted at a fixed displacement rate of 0.5 mm min^{-1}.

The longitudinal strain at the beginning of an interlaminar crack and the longitudinal strain at rupture are both read from experimental plots and are displayed in Table 3. The beginning of delamination leads to a brutal rupture of the specimen in the ±22.5° ply-based laminates, whereas the propagation of delamination at the mid-plane of the first laminate is progressive up until rupture.

Prediction

For the computation of delamination initiation, a specialized software EDA has previously been developed in the LMT Laboratory [33]. It solves the problem posed in a strip perpendicular to the edge, with the damage being located in the interfaces. In order to analyse E.D.T. specimens, the same type of approach was used in [34]. Knowing the parameters identified from the last section (see Table 1), we are then faced with having to choose an initial set for the other parameters *n* and the interlaminar stiffness values.

For the energy threshold Y_o, we initially assume that: $Y_o = 0$. Without any further information, we can choose $n = 0.5$, which is the value found for the single-layer. The stiffness values remain to be determined. A ±θ interface is assumed to be equivalent to a thin resin layer of two fiber diameters in thickness [29], or about 10 μm. From the properties of a standard epoxy resin, we can set a value of 4.10^5 N mm^{-3} for the normal stiffness and 10^5 N mm^{-3} for the shear stiffnesses. A 0°/0° interface physically resembles a transverse plane of a unidirectional layer. Knowing the rupture stresses measured in previous layer tests, we can identify the stiffness values of this interface from the local instability criterion. For instance, the stiffness value k_3^0 is set at 10^4 N mm^{-3} with σ_{33max} = 41 MPa.

From the initial set of parameters presented in Table 2 (Set 1), the predicted value of longitudinal strain at the initiation of delamination is displayed in Table 3. For two of the laminates tested, the predicted value is not very close to the experimental results, but in all cases, the delamination locus has been predicted exactly. A second set of parameters from Table 2 (Set 2) yields predictions that are closer to the experimental values (see Table 3) and that could be easily improved. Nevertheless, the discrepancies between computation and experimental results can be explained by the fact that this simulation doesn't take into account the damage occurring inside the layers, which is significant near the edges. Moreover, the beginning of edge delamination is often an unstable phenomenon which is not easy to detect with accuracy.

Table 2. Parameter sets (*in italics*: already identified).

Interface	Set n°	Y_c	γ_1 (= γ_2)	α	k_3^0	k_1^0 (= k_2^0)	n
0°/0°	Set 1	*0.11 N mm^{-1}*	*0.4*	*1.6*	1.10^4 N mm^{-3}	4.10^4 N mm^{-3}	0.5
	Set 2	"	"	"	4.10^5 N mm^{-3}	4.10^5 N mm^{-3}	0.2
± θ	Set 1	*0.18 N mm^{-1}*	*0.4*	*1.2*	4.10^5 N mm^{-3}	1.10^5 N mm^{-3}	0.5
	Set 2	"	"	"	4.10^4 N mm^{-3}	3.10^4 N mm^{-3}	0.5

Table 3. Simulated and experimental longitudinal strain at initiation of EDT specimens.

Laminate	Interface(s)	Mode	$\varepsilon_{rupture}$ (%) (number of specimens)	$\varepsilon_{ini\text{-}experiment}$ (%) (number of specimens)	$\varepsilon_{ini\text{-}prediction}$ (%)	
					Set 1	Set 2
$[0_3/\pm45_2/90]_s$	90°/90°	I	0.54 (3)	0.20 (3)	0.43	0.25
$[\pm22.5]_{4s}$	±22.5° (first)	II	0.64 (5)	0.60 (2)	0.96	0.81
$[0_4/\pm22.5_2]_s$	±22.5°	mixed	0.52 (3)	0.51 (1)	0.50	0.48

AN INITIAL IDENTIFICATION USING PLATES WITH HOLES

The initial identification with classical tests is not reliable enough. The various problems raised in the preceding sections are essentially of two kinds: the intralaminar damage is not always sufficiently accounted for and the initiation process is unstable and remains not fully understood. According to the authors, more reliable delamination tests would be those conducted on laminated plates with a circular hole. The idea herein is to use the first parameter set identified previously as the initial data for a global identification using plates with holes.

During the test, the damage map is monitored by means of X-ray photography. Also of interest in this test is the valuable information being provided in terms of the shape and size of the delaminated area. The difficulty herein is that, due to the complexity of the state of stresses, interpretation of the test requires complex computations. For such tests, a specialized software DSDM (Delamination Simulation by Damage Mechanics) has previously been developed [20] for predicting delamination around initially-circular holes, with the intralaminar damage being taken into account in the analysis.

The laminates tested are the same as those presented in Table 3; a $[0_2/45/0_2/\text{-}45/90_2]_s$ was also tested. The specimens are 50 mm in width and 150 mm in gage length, and the hole diameter is 10 mm. The tests were conducted in tension on an INSTRON testing machine at a fixed displacement rate of 0.5 mm min^{-1}. Only the $[0_4/\pm22.5_2]_s$ and the $[0_3/\pm45_2/90]_s$ laminates have exhibited a significant delaminated area around the hole. This finding is surprising because the $[0_2/45/0_2/\text{-}45/90_2]_s$ is supposed to be very sensitive to delamination. This finding serves to demonstrate that the delamination phenomenon is heavily dependent on material properties.

In what follows, we present an initial comparison between the experimental observations in the $[0_3/\pm45_2/90]_s$ laminate loaded in tension and the computation. Figure 5 shows the evolution of the X-revealed damage map near the hole for an increasing applied load. The first

damage, appearing at 55% of rupture (Fig. 5a), is transverse cracking in 90°-plies near the hole, and matrix cracking in the 0°-plies tangent at the hole and in the fibre direction called "splitting". Delamination only begins at about 80% of rupture (Fig. 5b). Just before the rupture (Fig. 5c), the delaminated area is always found to be located between the splittings and developed in the 0°-direction with about two hole diameters in length.
Micrographies were performed and show that the damage is well-developed in several ways: splittings, transverse cracking not only in the 90°-plies but also in the ±45°-plies, multiple delamination at the 0°/+45°, ±45° and -45°/90° interfaces (Fig. 6).
From the computation, the splitting can be seen as a shear damage in the 0°-layer (see Fig. 7). In fact, when the first 0°-fibres near the hole crack, the local load is transferred by shear in the matrix at the adjacent fibres. The delaminated area computed in the 0°/+45° interface (or a ±22.5° interface oriented at 22.5°) is shown in Figure 8 as an example (the delaminated area corresponds to d = 1). In the same manner, the other interfaces Äexcept for the mid-plane Ä are found to be delaminated. In order to achieve a good comparison, we have not, for the time being, used those parameters identified previously and which have led to the prediction of no delamination. Different explanations for this feature are currently under consideration, and some progress is being hoped for shortly. Nevertheless, this last example shows that it is possible to determine stacking sequences for which, despite the relative brittle behaviour of M55J/M18 material, the onset and the propagation of delamination is sufficiently stable and the size of the delaminated area is wide enough to perform better comparisons between complex computations and experimental test results.

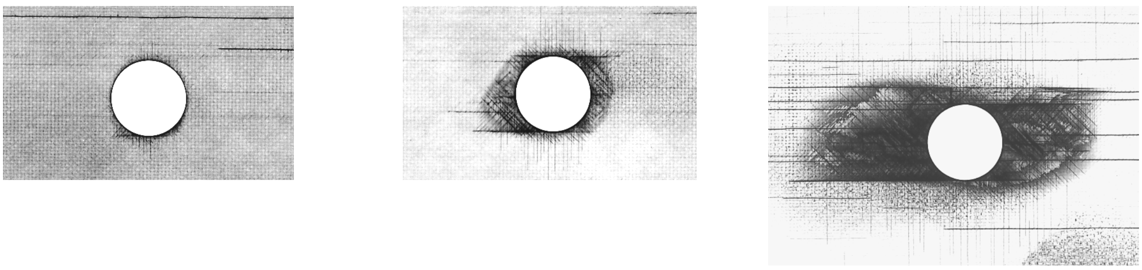

5a. 55% of rupture (237 MPa).

5b. 86% of rupture (370 MPa).

5c. 99% of rupture (426 MPa).

Fig. 5 : $[0_3/\pm45_2/90]_s$ X-ray damage map.

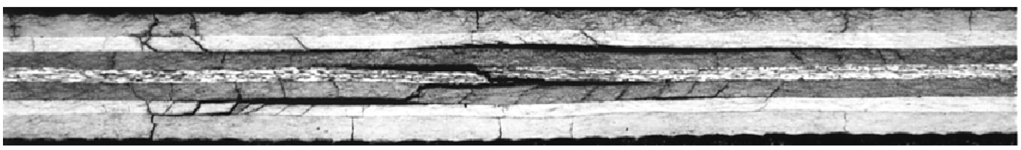

Fig. 6. : Micrograph of a section tangent to the hole of a $[0_3/\pm45_2/90]_s$ specimen at 92 % of the rupture load

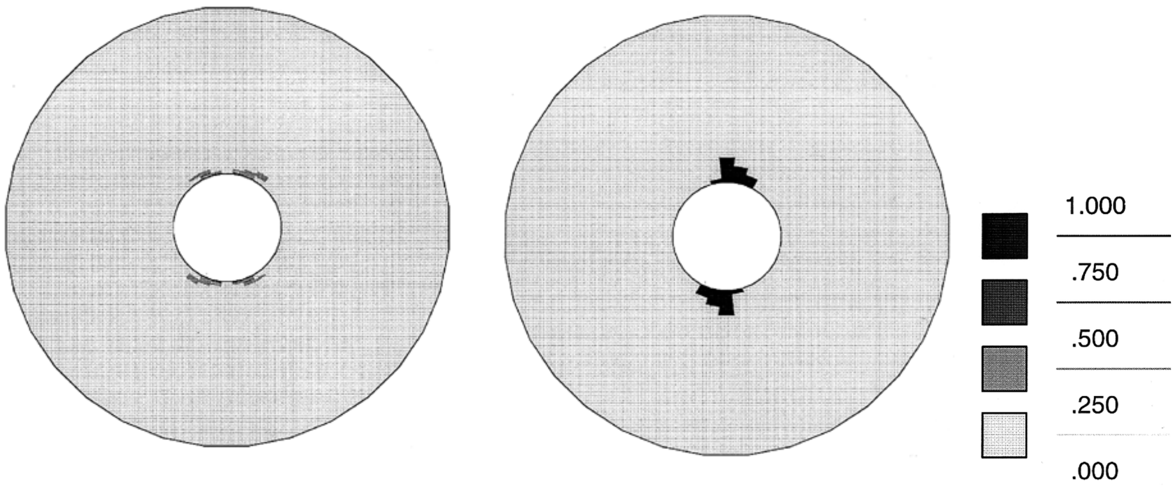

a) d indicator in the 0°-layers b) d' indicator in the 90°-layers c) value scale

Fig. 7 : Damage maps computed in the layers of a $[0_3/\pm45_2/90]_S$ holed-specimen at the rupture load

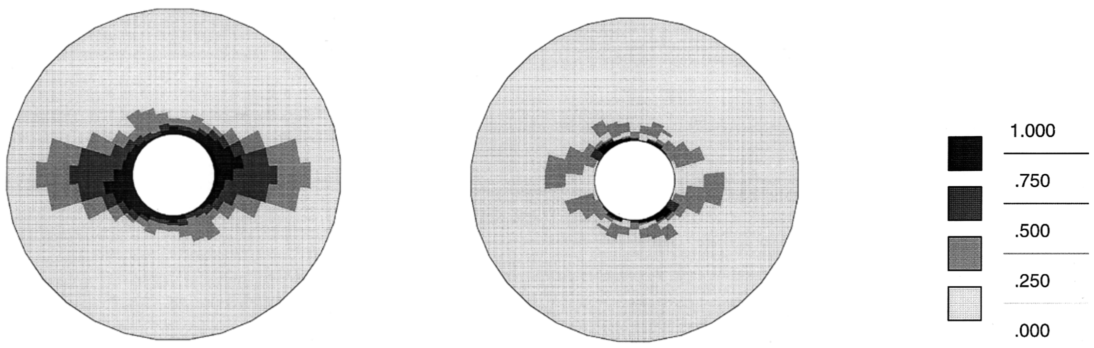

a) d_3 indicator at the ±45° interface b) d_3 indicator at the 0°/45° interface c) Äd$_i$Åvalue scale

Fig. 8 : Damage maps computed at the interfaces of a $[0_3/\pm45_2/90]_S$ holed-specimen at the rupture load

CONCLUSION

A meso-damage model of laminates, which includes the main deterioration mechanisms (transverse cracking, fiber breaking, delamination), has been described in detail. It is defined by a small set of intrinsic parameters. The approach used is quite advanced : the layer model and its identification have been completed. Due to the complexity of the phenomenon involved in what is called delamination, the interface identification is less advanced.

Nevertheless, links between Fracture Mechanics and Damage Mechanics allows obtaining a first sensible set of parameters. The interface model and its identification have been extended to the case of high viscosity [33]. Owing to our numerical and experimental background, the most important aspect to be developed at present, for a reliable identification of the interface model, concerns numerical simulation. The level of delamination obtained by simulation is in fact very sensitive to the numerical parameters (accuracy of the algorithm, size of the mesh, time step) [34]. The methods which allow controlling all of these parameters are currently under development.

ACKNOWLEDGEMENTS

The authors would like to thank M. Guédra Degeorges for enabling us to conduct these tests at the Centre Commun de Recherche Louis Blériot / AÉROSPATIALE in Suresnes, France.

REFERENCES

1. Highsmith, A.L. and Reifsnider K.L., "Stiffness reduction mechanism in composite material", In: ASTM-STP 775, Damage in Composite Materials, A.S.T.M., 1982, pp.103-117.
2. Talreja R., "Transverse cracking and stiffness reduction in composite laminates", Journal of Composite Materials, vol.19, 1985, pp. 355-375.
3 Kim, R.Y. & Soni S.R., "Experimental & analytical studies on the onset of delamination in laminated composites". J. Comp. Mater., 18, 1984, p. 70-80.
4 Engrand, D., "Calcul des contraintes de bords libres dans les plaques composites symétriques avec ou sans trou. Comparaison avec l'expérience". Comptes Rendus des Troisièmes Journées Nationales sur les Composites, Paris, 1982, pp 289-297.
5 Leguillon, D. and Sanchez-Palancia E., "Effets de bords et singularités dans les matériaux composites". Annales des Composites, Effets de bords et singularités dans les matériaux composites stratifiés, AMAC, Chatenay-Malabry, 1987, pp 7-20.
6 De Charentenay, F.-X., Harry J.M., Prel Y.J. and Benzeggagh M.L., "Characterizing the Effect of Delamination Defect by Mode I Delamination Test. Effect of Defects in Composite Materials", ASTM STP 836, 1984, pp 84-103.
7 Davies, P. & al. "Measurement of G_{Ic} and G_{IIc} in Carbon/Epoxy Composites". Comp. Sci. & Technol., 39, 1990, pp. 193-205.
8 Leguillon, D., "Le critère de Griffith appliqué à l'amorçage d'une fissure". Actes du troisième colloque national en calcul des structures, CSMA/ECN, Presses Académiques de l'Ouest, Giens, mai 1997.
9. Garg C. A., "Delamination. A damage mode in composite structures". Engineering Fracture Mechanics, Vol 29, n 5, 1988, pp. 557-584.
10. Whithney, J.M., "Experimental characterization of delamination fracture". In Interlaminar response of composite materials, Comp.Mat. Series, 5, Pagano, N. J. ed, 1989, pp.111-239.
11. Ladevèze, P., "Sur la Mécanique de l'Endommagement des composites". In Comptes rendus des JNC 5, C. Bathias & D. Menkès eds, Pluralis Publication, Paris, 1986, pp. 667-683.
12. Ladevèze, P., "A damage computational method for composite structures", J. Computer and Structure, 44 (1/2), 1992, pp. 79-87.
13. Ladevèze P., and Le Dantec, E., "Damage modeling of the elementary ply for laminated composites", Composite Science and Technology, 43-3, 1992, pp.257-267.
14. Allix, O., and Ladevèze, P., "Interlaminar interface modelling for the prediction of laminates delamination"., Composite Sructures 22, 1992, pp. 235-242.
15. Allix, O., and Ladevèze, P., "A meso-modelling approach for delamination prediction". In Fracture and Damage in Quasibrittle Structures. Bazant, Z. P., Bittnar, Z., Jirasek, M. eds, 1994, pp. 606-15.

16. Allix, O. , Levêque, D., and Perret, L., "Interlaminar interface model identification and forecast of delamination in composite laminates" Composite Science & Technology Vol. 58-5 1998, pp 671-678.
17. Corigliano, A., "Formulation, identification and use of interface models in the numerical analysis of composite delamination". Int.J. Solids Structures, 30, 1993, 2779-2811.
18. Allix, O., and Ladevèze P. & Corigliano A., "Damage analysis of interlaminar fracture specimens". Composite Sructures, 31, 1995, pp. 61-74.
19. Allix, O. & Corigliano A., "Modeling and simulation of crack propagation in mixed-mode interlaminar fracture specimens". Int. J. of Fracture, 77, 1996, pp.111-140.
20. Allix, O., "Damage analysis of delamination around a hole". New Advances in Computational Structural Mechanics, P. Ladevèze, O. C. Zienkiewicz Eds., Elsevier Science Publishers B. V., 1992, pp. 411-421.
21 Allix, O. , Levêque, D., Technical report. CNES (French National Center for Space Studies) n 840/CNES/94/1406/00, January 1996.
22. Pijaudier-Cabot, G. and Bazant, Z.P. , "Nonlocal damage theory", ASCE J. Eng. Mech., 113, 1987, pp.1512-1533 .
23. Lasry, D. and Belytschko, T. , "Localization limiters in transient problems", Int. J. Solids Struct., 24, 1988, pp. 581-597.
24. Ladevèze P., "Towards a Fracture Theory", Proceedings of the third International Conference on computational Plasticity Part II, D.R.J. Owen, E. Onate, E. Hinton ed, Pineridge press, Cambridge U.K., 1992, pp. 1369-1400.
25. Allix, O., Ladevèze, P., and Vittecoq E., "Modelling and Identification of the mechanical behaviour of composite laminates compression", Composite Science & Technology Vol 51-1, 1994, pp. 35-42.
26. Allix, O., Guédra-Degeorges D., Guinard S.,and Vinet A., "3D damage analysis for analyzing low energy impact on impact on composite laminates", ICCM12 12th Int. Conf. on Comp. Mat. Paris Juillet 99
27. Guédra Degeorges, D., "Principaux essais de délaminage - exploitation". Une nouvelle approche des composites par la Mécanique de l'Endommagement, Cachan, 1993, pp 229-249.
28. Russell, A.J. and Street K.N., "Moisture and Temperature Effects on the Mixed-Mode Delamination Fracture of Unidirectional Graphite/Epoxy, Delamination and Debonding of Materials", ASTM STP 876, W.S. Johnson, Ed., Philadelphia, 1985, pp 349-370.
29. Billoët, J.-L., Ben Zineb T., and Ben Lazreg B., "Introduction de l'effet de paroi dans l'analyse des contraintes de bords libres pour les plaques stratifiées". C. R. des JNC 9, AMAC, Saint-Étienne, J.-P. Favre & A. Vautrin, Editors. Nov. 1994, pp. 833-842, 22-24 .
30. O'Brien, T.K., "Characterization of Delamination Onset and Growth in a Composite Laminate". Damage in Comp. Mat., ASTM STP 775, Reifsnider, Ed., 1982, pp 140-167.
31. Kim, R.Y., "Experimental Observations of Free-Edge Delamination". In Interlaminar Response of Composite Materials, N.J. Pagano Ed., 1989, pp 111-160.
32. Crossman, F.W. and Wang, A.S.D., "The Dependence of Transverse Cracking and Delamination on Ply Thickness in Graphite/Epoxy Laminates". Damage in Composite Materials, ASTM STP 775, K.L. Reifsnider, Ed., 1982, pp 118-139.
33. Daudeville, L. and Ladevèze, P., "A Damage Mechanics Tool for Laminate Delamination", Journal of Composite Structures n∞25, 1993, pp. 547-555.
34. Schellekens, J.C. and De Borst, R., "A non-linear finite element approach for the analysis of mode I-free edge delamination in composites". Int. Journal Solids Structures, vol. 30-9, 1993, pp.1239-53.
35. Corigliano., A.and Frassina R., "Rate dependent fracture properties in the delamination of polymer-matrix composites". IV World Congress on Computational Mechanics, Buenos Aires, Argentina, June 29-July 2, 1998.